

Supporting information for:

**Influence of Morphology on Blinking Mechanisms
and Excitonic Fine Structure of Single Colloidal
Nanoplatelets**

Zhongjian Hu,[†] Ajay Singh,[†] Serguei V. Goupalov,^{‡,¶} Jennifer A. Hollingsworth,[†]
and Han Htoon^{*,†}

[†]*Center for Integrated Nanotechnologies, Material Physics and Applications Division, Los
Alamos National Laboratory, Los Alamos, NM 87545*

[‡]*Department of Physics, Jackson State University, Jackson, Mississippi 39217, USA*

[¶]*Ioffe Institute, 194021 St. Petersburg, Russia*

E-mail: htoon@lanl.gov

Supplementary Note 1: Synthesis of nanoplatelets

Materials

Cadmium acetate hydrate (≥ 99.99 %, Aldrich), oleic acid (90 %, Aldrich), 1-octadecene (90 %, Aldrich), selenium (powder, 99.99 %, Aldrich), sulfur (powder, 99.998 %, Aldrich), zinc nitrate hydrate (99.99 %, Aldrich), ammonium sulfide solution (40-48 wt. % in H₂O, Aldrich), octylamine (99 %, Aldrich), and N-methylformamide (99 %, Aldrich) were used as received.

CdSe Nanoplatelets Synthesis

CdSe NPLs with emission around 555 nm are synthesized according to previously published procedure with slight modifications.^{S1} In a three neck round bottomed flask, cadmium myristate (0.172 g) and 1-octadecene (14 mL) are loaded. The reactants are degassed under vacuum for 30-40 minutes at room temperature and then ramp to 250°C under argon environment. When the temperature is stabilized at 250°C, a pre-stirred mixture of selenium (0.019 g) in 1-octadecene (1 mL) is injected into the reaction flask. After 1 min, 0.120 g of cadmium acetate dehydrate is added quickly and reaction is kept at 250°C for another 10-12 min. After cool down to room temperature, 0.6 mL of oleic acid was added to the flask. The solution was centrifuged at 5000 rpm and precipitated nanoplatelets are redispersed in hexane. The nanoplatelets are further washed twice using ethanol for precipitation and re-dispersing in hexane.

CdSe/CdZnS Core shell (Smooth) Nanoplatelets

Smooth shell NPLs were synthesized following atomic layer deposition approach with some modification.^{S2} Typically, 500 μ L of as-synthesized CdSe NPLs (555 nm) are diluted in 4.5 mL hexane and then added to 5 mL of N-methylformamide (NMF). 50 μ L of ammonium sulfide solution is added to this mixture. The mixture is vortexed/stirred continuously

for 2-3 minutes, which results in the phase-transfer of NPLs in the polar phase (NMF) through ligand exchange. Next, the polar phase is washed 2-3 times with hexane. After that, NPLs are precipitated using toluene and acetonitrile mixture (3:1) and redispersed into 2 mL of NMF. To put the first CdZn (cationic layer), 2.5 mL of a 0.1 M solution composed of $(\text{Cd}(\text{OAc})_2 \cdot x\text{H}_2\text{O})$, 1.875 mL) and $(\text{Zn}(\text{NO}_3)_2 \cdot \text{H}_2\text{O})$, 0.625 mL) in NMF with a fixed $\text{Cd}^{2+}/\text{Zn}^{2+}$ ratio (7.5:2.5) is added. The mixture is vortex/stirred for 2-3 minutes. The mixture is again washed with toluene and acetonitrile mixture and redispersed into 1 mL of hexane. These steps were repeated twice more to get final 3 ML of CdZnS on CdSe core. After final layer deposition, the NPLs are dispersed in hexane containing $\text{Cd}(\text{oleate})_2$ (0.02mmol) and the excess ligand is removed by precipitation with ethanol. The final precipitate is dispersed in hexane and used as it for further analysis.

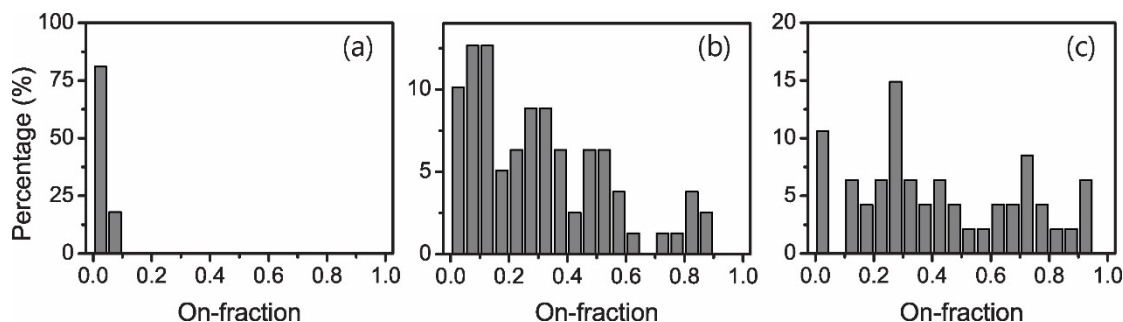
CdSe/CdZnS Core shell (Rough) Nanoplatelets

To achieve rough shell, we used previously published continuous shell growth protocol with minor modification.^{S3} In a 6 mL vial, 2 mL of chloroform is taken and 200 μL of as-synthesized CdSe NPLs in hexane are added into that. Next, 0.025 g of thioactamide and 300 μL of octylamine are added into the vial. This mixture is sonicated until thioactamide was completely dissolved. After that a solution of $\text{Cd}(\text{NO}_3)_2$ and $\text{Zn}(\text{NO}_3)_2$ in ethanol solution (0.2 M) is introduced into the vial and the reaction was left at room temperature to proceed for 18 hours. The resulting core-shell NPLs are precipitate using excess ethanol and then redispersed in chloroform containing $\text{Cd}(\text{oleate})_2$ (0.02mmol) solution. Finally, this solution is precipitated using ethanol to remove the excess ligand and then re-suspended in chloroform.

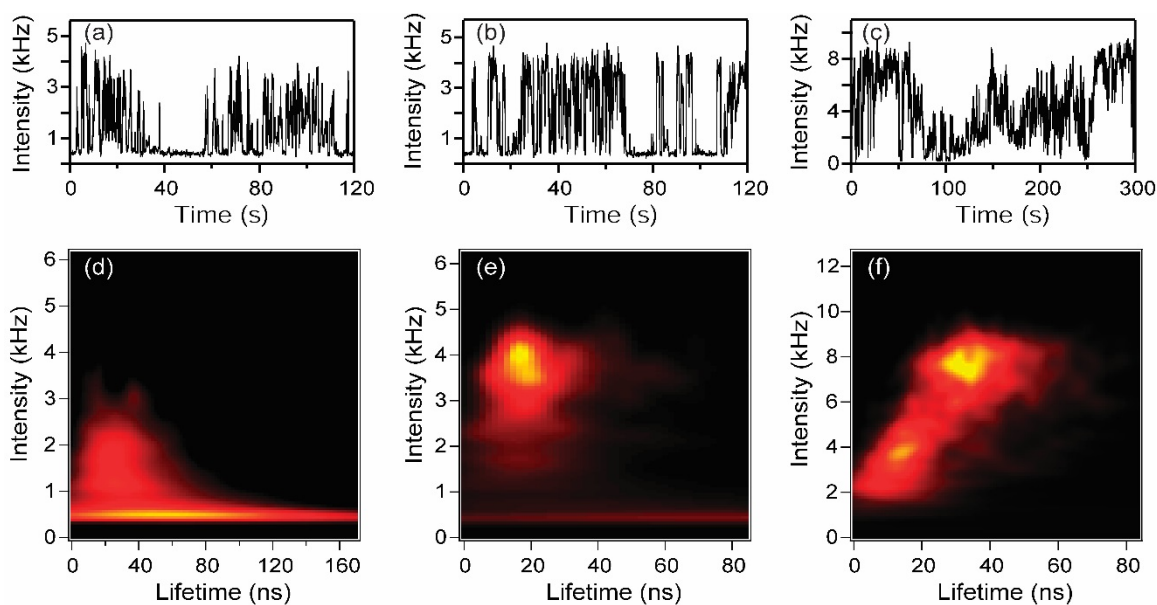
Supplementary Note 2: Experimental Details

Structural and Optical Characterization

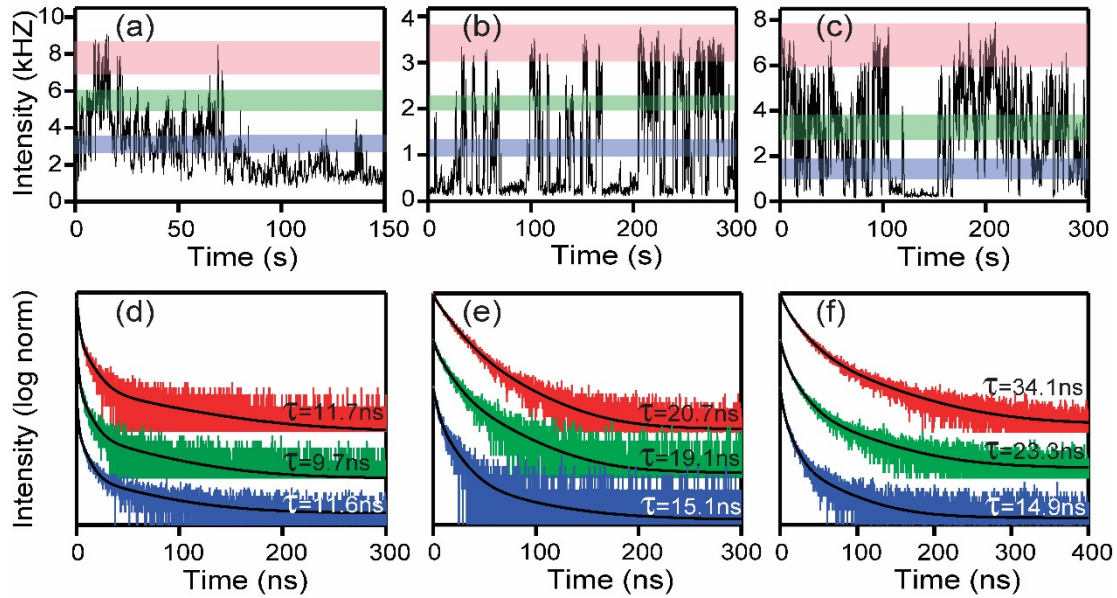
Transmission electron microscopy (TEM) images were obtained using a FEI Tecnai transmission electron microscope operating at 300 kV. Absorption and emission spectra were collected using a Cary Varian 5000 UV-Vis-NIR spectrophotometer and a Horiba NanoLog spectrofluorometer, respectively. The statistical photostability analysis of the on-time fraction of single NPLs was performed. In this kind of experiment, a one-hour wide-field PL movie (under continuous excitation under 5 W/mm^2) is taken first, from which the PL intensity blinking traces for individual NPLs are extracted using an Igor routine. Then, the intensity traces are analyzed by setting a threshold level at 3 standard deviations above the average background signal, above which the PL is considered to be on and below which is taken as off. One value of on-time fraction is obtained for one NPL analyzed. Fig. S1 demonstrates distributions of on-time fraction of ~ 50 single NPLs for each type of NPLs in three panels respectively.



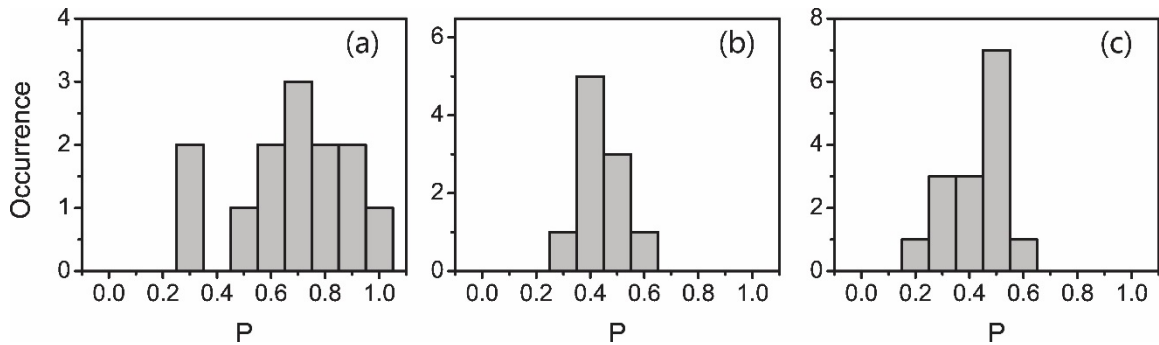
Supplementary Figure S1: Photoluminescence on-fraction distribution histograms for NPLs over 1-hour illumination under 5 W/mm^2 : (a) CdSe core NPLs, (b) smooth shell CdSe/CdZnS NPLs, and (c) rough shell CdSe/CdZnS NPLs. It can be seen that when going from the core NPLs to the NPLs with shell (irrespective of the shell morphology) the on-time fraction increases significantly.



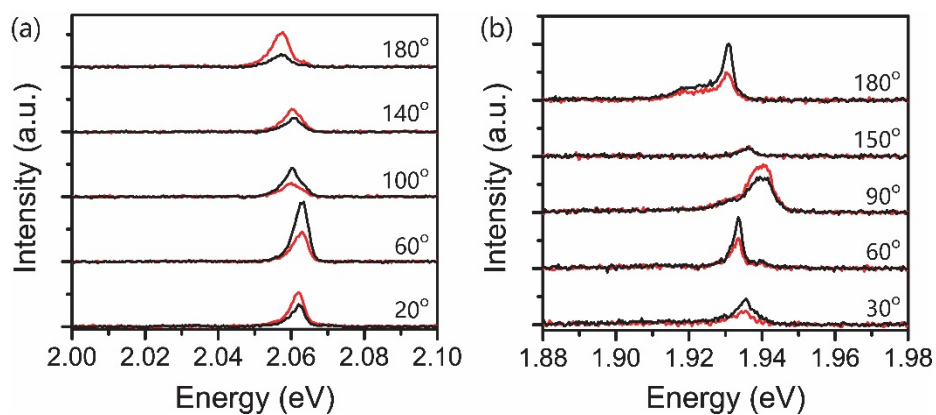
Supplementary Figure S2: An extra dataset of PL intensity time traces of single core CdSe NPL (a), smooth-shell CdSe/CdZnS NPL (b), and rough-shell CdSe/CdZnS NPL (c). Panels (d-f) display the FLID diagrams for the corresponding time traces (a-c), respectively.



Supplementary Figure S3: Representative photoluminescence intensity time traces (same as the traces shown in Figure 2 in the main text) of the core CdSe NPLs (a), the smooth shell NPLs (b), and the rough shell NPLs (c). Panel (d-f) display the PL decays for three different intensity bands highlighted in the corresponding time traces (a-c) for three types of NPLs, respectively. The decay fits (black traces) and the fitted lifetimes (inset τ values) for each decay are shown in (d-f). As shown, the three different intensity levels for the core NPLs (d) and the smooth shell NPLs (e) exhibit similar PL lifetime. In contrast, the rough shell NPLs demonstrate distinct behavior: as shown in (f), the PL lifetime decreases with the drop of PL intensity.



Supplementary Figure S4: Distribution histograms of room-temperature degree of PL emission polarization for (a) CdSe core NPLs, (b) smooth shell CdSe/CdZnS NPLs, and (c) rough shell CdSe/CdZnS NPLs.



Supplementary Figure S5: Representative polarization-resolved spectra at 10 K collected at different emission detection angles for (a) a smooth-shell CdSe/CdZnS NPL and (b) a rough-shell CdSe/CdZnS NPL. As shown, at low temperature the spectra detected in two orthogonal channels have analogous spectral profile, meaning that there is no detectable fine structure splitting.

Supplementary Note 3: Theory

Anisotropic exchange splitting

We consider a CdSe colloidal nanoplatelet of the width $L_z = 30 \text{ \AA}$ with a rough shell. We suppose that an exciton as a whole can get localized on the island of shell roughness and estimate the resulting anisotropic splitting. We assume that the exciton is localized on the length $2L_y = 70 \text{ \AA}$ in the y -direction and will vary its localization length along the x -direction which has the size of the surface roughness.

We will start with the well-known expression for the exciton resonance frequency renormalization due to the long-range electron-hole exchange interaction, $\delta\omega_0^{(\alpha)}$ and the exciton radiative lifetime, τ_α for heavy-hole excitons localized in quantum wells^{S4,S5}

$$\delta\omega_0^{(\alpha)} - i(2\tau_\alpha)^{-1} = \omega_{LT}\pi a_B^3 S^{-1} \sum_{\mathbf{q}} T_\alpha(\mathbf{q}) F^2(\mathbf{q}), \quad (1)$$

$$T_\alpha(\mathbf{q}) = \frac{i}{2} \frac{q_\alpha^2 - k^2}{k_z} \int \int dz dz' \Phi(z) \Phi(z') e^{ik_z|z-z'|}, \quad (2)$$

where the index α indicates the polarization of the exciton sublevels, ω_{LT} and a_B are the longitudinal-transverse splitting and the Bohr radius of a free exciton in the bulk material, respectively, k is the light wavevector inside the medium at the exciton resonance frequency ω_0 , \mathbf{q} is the two-dimensional vector (q_x, q_y) , $k_z = \sqrt{k^2 - q^2}$, $\Phi(z) = \varphi_{e1}(z)\varphi_{hh1}(z)$ is the product of the electron and hole envelope wave functions along the axis of the quantum well or nanoplatelet, $F(\mathbf{q}) = \int d\vec{\rho} \exp(-i\mathbf{q}\vec{\rho}) \psi(\vec{\rho}, \vec{\rho})$, S is the normalization area. Here $\psi(\vec{\rho}, \vec{\rho})$ is the exciton envelope wave function at the coinciding coordinates of the electron and the hole. We will follow Ref.^{S5} and take the latter in the form

$$\psi(\vec{\rho}, \vec{\rho}) = \frac{2}{\pi \tilde{a} \sqrt{L_x L_y}} \exp\left(-\frac{X^2}{L_x^2} - \frac{Y^2}{L_y^2}\right),$$

where \tilde{a} is the effective two-dimensional Bohr radius. Then, if all the sizes are less than the

wavelength of light, one can take the limit of negligible light wave vector ($k \rightarrow 0$) and write the following expressions for the exchange-induced resonance frequency renormalizations:

$$\delta\omega_0^{(x)} \approx \frac{\omega_{LT} a_B^3 L_x L_y}{2\pi \tilde{a}^2} \int_0^\infty dt t^2 \int_0^{2\pi} d\varphi \cos^2 \varphi e^{-t^2 \cos^2 \varphi L_x^2/2} e^{-t^2 \sin^2 \varphi L_y^2/2} \quad (3)$$

$$\times \int dz \Phi(z) \int dz' \Phi(z') e^{-t|z-z'|},$$

$$\delta\omega_0^{(y)} \approx \frac{\omega_{LT} a_B^3 L_x L_y}{2\pi \tilde{a}^2} \int_0^\infty dt t^2 \int_0^{2\pi} d\varphi \sin^2 \varphi e^{-t^2 \cos^2 \varphi L_x^2/2} e^{-t^2 \sin^2 \varphi L_y^2/2} \quad (4)$$

$$\times \int dz \Phi(z) \int dz' \Phi(z') e^{-t|z-z'|}.$$

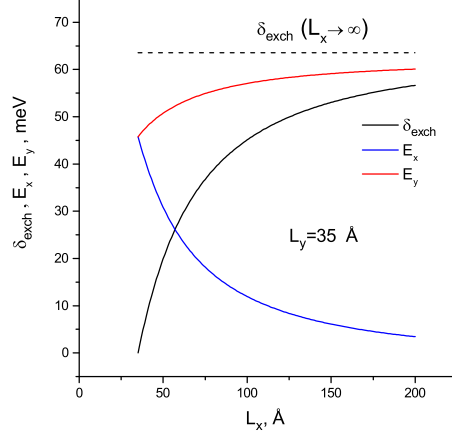
The difference of Eqs. (4) and (3) gives the equation from the main text.

In Refs. [S4,S5](#) equations similar to Eqs. (3), (4) were used to explain fine-structure splitting for heavy-hole excitons localized on islands of monolayer high interface fluctuations in GaAs/AlGaAs quantum wells. [S6](#) Fine-structure splittings on the order of 20 – 50 μeV are typically observed in that system. [S6](#) This results from a bulk exciton longitudinal-transverse splitting $\hbar\omega_{LT}^{\text{GaAs}} \approx 80 \mu\text{eV}$ and in-plane Bohr radius $\tilde{a}^{\text{GaAs}} \sim 80 \text{ \AA}$. For CdSe nanoplatelets we should use $\hbar\omega_{LT} = 0.95 \text{ meV}$ [S7](#) while the effective two-dimensional Bohr radius for excitons in nanoplatelets is known to be $< 10 \text{ \AA}$. [S8](#) Therefore, we can expect the fine-structure splitting 2 – 3 orders of magnitude larger than in GaAs/AlGaAs quantum wells.

For a more precise estimate we take

$$\Phi(z) = \frac{2}{L_z} \cos^2 \frac{\pi z}{L_z},$$

$a_B = 56 \text{ \AA}$, $\tilde{a} = 7 \text{ \AA}$. The resulting dependence of the anisotropic exchange splitting on the size of the localizing potential along x , L_x , at the fixed size along y , $L_y = 35 \text{ \AA}$, is shown in Supplementary Figure [S6](#) as a black solid line. The splitting is zero for $L_x = L_y$. Also shown in Supplementary Figure [S6](#) are $E_x = \hbar\delta\omega_0^{(x)}$ (blue solid line) and $E_y = \hbar\delta\omega_0^{(y)}$ (red



Supplementary Figure S6: Dependence of the anisotropic exchange splitting, $\delta_{exch} = \hbar \left(\delta\omega_0^{(y)} - \delta\omega_0^{(x)} \right)$, on the localization size along x , L_x (black solid line). The limit of the splitting for an exciton delocalized along x -direction is shown by dashed black line. The localization size along y -axis is fixed: $2L_y = 70 \text{ \AA}$. Also shown are size dependencies of $E_x = \hbar \delta\omega_0^{(x)}$ (blue solid line) and $E_y = \hbar \delta\omega_0^{(y)}$ (red solid line).

solid line).

In order to describe a delocalized exciton in the nanoplatelet one should substitute

$$F^2(\mathbf{q}) = \frac{2\sqrt{2}}{\sqrt{\pi}\tilde{a}^2} L_x L_y \delta_{q_x,0} e^{-q_y^2 L_y^2/2},$$

where L_x now denotes the full length of the nanoplatelet along the x axis, into eq. (1). This yields

$$\delta\omega_0^{(y)} \approx \sqrt{\frac{2}{\pi}} \frac{\omega_{LT} a_B^3 L_y}{\tilde{a}^2} \int_0^\infty dt t e^{-t^2 L_y^2/2} \int dz \Phi(z) \int dz' \Phi(z') e^{-t|z-z'|}. \quad (5)$$

For the parameters given above this gives $\hbar \delta\omega_0^{(y)} = 63.5 \text{ meV}$ while $\delta\omega_0^{(x)}$ for a delocalized exciton is zero. The corresponding δ_{exch} is shown in Supplementary Figure S6 as a dashed line.

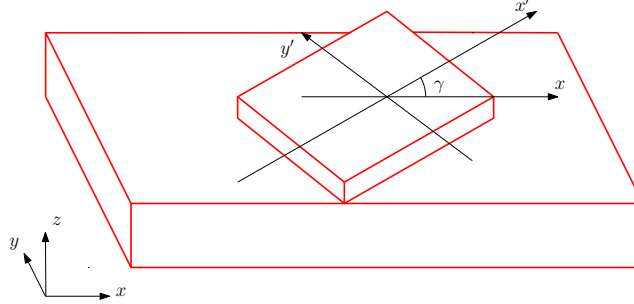
Note that Eq. (5) can be directly obtained from Eq. (4) as a limiting case of $L_x \rightarrow \infty$, if one rewrites the integral in the Cartesian coordinates $q_x = t \cos \varphi$, $q_y = t \sin \varphi$ and takes into account that

$$\frac{L_x}{\sqrt{2\pi}} e^{-L_x^2 q_x^2/2} \rightarrow \delta(q_x)$$

when $L_x \rightarrow \infty$.

PL Polarization

Let us suppose that orientation of the island with respect to the nanoplatelet is as shown in Supplementary Figure S7. Let us study how it would influence PL polarization. As the



Supplementary Figure S7: Possible orientation of the island.

size of the nanoplatelet is much less than the wavelength of light which is used to excite PL, one can use the description of the electric fields as in electrostatic theory.^{S9} We will suppose that the main axes of the island (x' , y') form the angle γ with respect to the main axes of the nanoplatelet (x , y). We will assume that the shape and orientation of the island determine the directions of the emitting dipoles while all depolarization effects are due to the nanoplatelet itself.

Let us suppose that we are measuring intensity of the linearly polarized light and that the axis describing polarization of our analyzer forms the angle θ with respect to the long axis of the nanoplatelet, x .

If the emitting dipole is oriented along the x' axis ($\mathbf{d}||x'$) then the measured light intensity

$$I_{||}^{x'}(\theta) \propto (k_l \cos \theta \cos \gamma + k_t \sin \theta \sin \gamma)^2, \quad (6)$$

where k_l and k_t are the depolarization factors. If $k_l = k_t$ then $I_{||}^{x'}(\theta) \propto \cos^2(\theta - \gamma)$. The

total intensity

$$I_{\parallel}^{x'} + I_{\perp}^{x'} \propto (k_l^2 \cos^2 \gamma + k_t^2 \sin^2 \gamma). \quad (7)$$

If the emitting dipole is oriented along the y' axis ($\mathbf{d} \parallel y'$) then the measured light intensity

$$I_{\parallel}^{y'}(\theta) \propto (k_t \sin \theta \cos \gamma - k_l \cos \theta \sin \gamma)^2. \quad (8)$$

If $k_l = k_t$ then $I_{\parallel}^{y'}(\theta) \propto \sin^2(\theta - \gamma)$. The total intensity

$$I_{\parallel}^{y'} + I_{\perp}^{y'} \propto (k_t^2 \cos^2 \gamma + k_l^2 \sin^2 \gamma). \quad (9)$$

For an estimate it is convenient to model the nanoplatelet as an ellipsoid with the semi-axes a , b , and c . Then the depolarization factors k_l and k_t are given by^{S10}

$$k_l = \left[1 + \left(\frac{\varepsilon_i}{\varepsilon_e} - 1 \right) n_x \right]^{-1}, \quad (10)$$

$$k_t = \left[1 + \left(\frac{\varepsilon_i}{\varepsilon_e} - 1 \right) n_y \right]^{-1}, \quad (11)$$

where ε_i (ε_e) is the dielectric constant inside (outside) the ellipsoid on the frequency of the excitonic resonance, and n_x and n_y are the depolarization coefficients.^{S10} These coefficients can be obtained as^{S10}

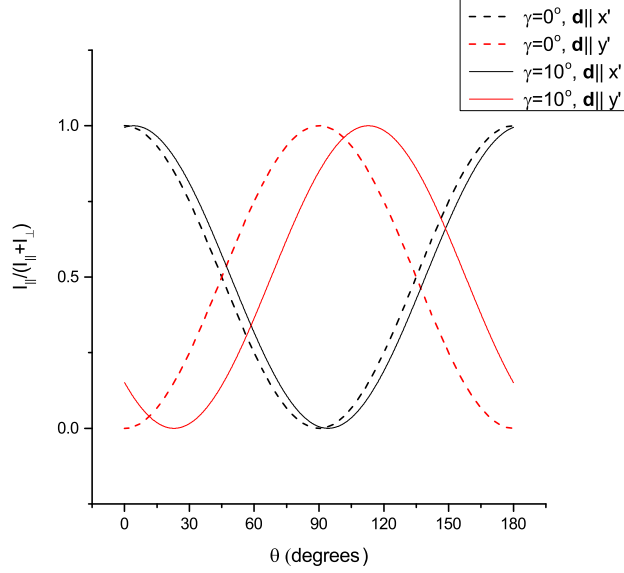
$$n_x = \frac{abc}{2} \int_0^{\infty} \frac{ds}{(s+a^2)^{3/2} (s+b^2)^{1/2} (s+c^2)^{1/2}}, \quad (12)$$

$$n_y = \frac{abc}{2} \int_0^{\infty} \frac{ds}{(s+a^2)^{1/2} (s+b^2)^{3/2} (s+c^2)^{1/2}}. \quad (13)$$

We describe the nanoplatelet as an ellipsoid with the semi-axes $a = 250 \text{ \AA}$, $b = 35 \text{ \AA}$, and $c = 17.5 \text{ \AA}$. This gives $n_x = 0.01945$, $n_y = 0.32438$ ¹. For the dielectric constants we

¹ n_z can be defined similarly to n_x and n_y . Then $n_x + n_y + n_z = 1$ holds^{S10} which allows one to calculate

take $\varepsilon_i = 6$, $\varepsilon_e = 1$.

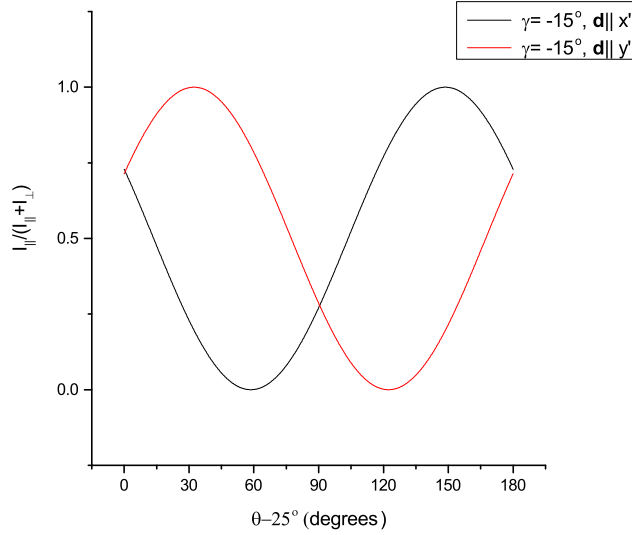


Supplementary Figure S8: Angular dependencies of $I_{\parallel}^{x'}(\theta)/(I_{\parallel}^{x'} + I_{\perp}^{x'})$ (black lines) and $I_{\parallel}^{y'}(\theta)/(I_{\parallel}^{y'} + I_{\perp}^{y'})$ (red lines) for $\gamma = 0^\circ$ (dashed lines) and $\gamma = 10^\circ$ (solid lines).

In Supplementary Figure S8 are shown the angular dependencies of $I_{\parallel}^{x'}(\theta)/(I_{\parallel}^{x'} + I_{\perp}^{x'})$ and $I_{\parallel}^{y'}(\theta)/(I_{\parallel}^{y'} + I_{\perp}^{y'})$ for $\gamma = 0^\circ$ (dashed lines) and $\gamma = 10^\circ$ (solid lines). While for $\gamma = 0^\circ$ (dashed lines) the phase shift for x' - and y' - polarized dipoles is 90° , for $\gamma = 10^\circ$ (solid lines) it is $\sim 60^\circ$. Supplementary Figure S8 also reveals that, at small γ , emission along x' is almost unaffected by depolarization effects (see also Figure 5 (d) of the main text).

In Supplementary Figure S9 are shown the angular dependencies of $I_{\parallel}^{x'}(\theta)/(I_{\parallel}^{x'} + I_{\perp}^{x'})$ and $I_{\parallel}^{y'}(\theta)/(I_{\parallel}^{y'} + I_{\perp}^{y'})$ for parameters chosen to closely reproduce the experimentally observed dependencies presented in Figure 4 (e) of the main text (see also Figure 5 (d) of the main text). It is assumed that the emitted light is 100 % linearly polarized.

n_x , n_y , and n_z numerically with a controllable precision.



Supplementary Figure S9: Angular dependencies of $I_{\parallel}^{x'}(\theta) / (I_{\parallel}^{x'} + I_{\perp}^{x'})$ (black solid line) and $I_{\parallel}^{y'}(\theta) / (I_{\parallel}^{y'} + I_{\perp}^{y'})$ (red solid line) for $\gamma = -15^\circ$.

References

- (S1) Ithurria, S. et al. Colloidal nanoplatelets with two-dimensional electronic structure. *Nature Materials* **2011**, 10 (12), 936–941.
- (S2) Tessier, M.D. et al. Spectroscopy of Colloidal Semiconductor Core/Shell Nanoplatelets with High Quantum Yield. *Nano Letters* **2013**, 13 (7), 3321–3328.
- (S3) Mahler, B; Nadal, B.; Bouet, C.; Patriarche, G.; Dubertret, B. Core/Shell Colloidal Semiconductor Nanoplatelets. *Journal of the American Chemical Society* **2012**, 134 (45), 18591–18598.
- (S4) Gupalov, S.V.; Ivchenko, E.L.; Kavokin, A.V. Fine structure of localized exciton levels in quantum wells, *J. Exp. Theor. Phys.* **1998**, 86 (2), 388–394.
- (S5) Goupalov, S.V.; Ivchenko, E.L.; Kavokin, A.V. Anisotropic exchange splitting of excitonic levels in small quantum systems. *Superlatt. Microstruct.* **1998**, 23 (6), 1205–1209.
- (S6) Gammon, D.; Snow, E.S.; Shanabrook, B.V., Katzer, D.S.; Park, D. Fine Structure

- Splitting in the Optical Spectra of Single GaAs Quantum Dots. *Phys. Rev. Lett.* **1996**, 76 (16), 3005–3008.
- (S7) Kiselev, V.A.; Razbirin, B.S.; Uraltsev, I.N. Additional Waves and Fabry-Perot Interference of Photoexcitons (Polaritons) in Thin II-VI Crystals. *Phys. Stat. Sol. (b)* **1975**, 72 (1), 161–172.
- (S8) Benchamekh, R.; Gippius, N.A.; Even, J.; Nestoklon, M.O.; Jancu, J.-M.; Ithurria, S.; Dubertret, B.; Efros, Al.L.; Voisin, P. Tight-binding calculations of image-charge effects in colloidal nanoscale platelets of CdSe. *Phys. Rev. B* **2014**, 89 (3), 035307.
- (S9) Lavallard, P.; Suris, R.A. Polarized Photoluminescence of an Assembly of Non-cubic Microcrystals in a Dielectric Matrix. *Sol. St. Commun.* **1995**, 95 (5), 267–269.
- (S10) Landau, L.D.; Lifshits, E.M. *Electrodynamics of continuous media*, 2nd Ed. (Elsevier, Amsterdam 1984).